

Surface Analysis during Plasma Etching by Laser-Induced Thermal Desorption

Irving P. HERMAN, Vincent M. DONNELLY¹, C.-C. CHENG^{1,*} and Keith V. GUINN¹

Department of Applied Physics and Columbia Radiation Laboratory, Columbia University, New York, NY 10027, U.S.A.

¹Bell Laboratories, Lucent Technologies, Murray Hill, New Jersey 07974, U.S.A.

(Received October 30, 1995; accepted for publication December 22, 1995)

The use of laser desorption (LD) to desorb species from the surface and laser-induced fluorescence (LIF) to detect them in the gas phase during etching of Si(100) in a high-charge-density plasma of Cl₂ and Cl₂/HBr mixtures is reviewed. The LD-LIF intensities of SiCl and SiBr are used to track the surface coverages of SiCl_{x(ads)} and SiBr_{x(ads)}, respectively, as a function of RF power, DC bias, and partial pressure, and as a function of time when the plasma is turned on and off. In-line X-ray photoelectron spectroscopy (XPS), the use of which is validated by these *in situ* LD-LIF studies, is employed after etching to calibrate the surface coverages obtained from the LD-LIF measurements.

KEYWORDS: plasmas, plasma etching, Si, Cl₂, HBr, laser desorption, laser-induced fluorescence (LIF), XPS, optical diagnostics

1. Introduction

Despite considerable effort, plasma etching mechanisms are still not well understood. In particular, deviations from ideal anisotropic etching are often observed and are the subject of many current investigations. Most experimental and theoretical studies have dealt with the gas-phase plasma physics and chemistry. Fewer studies have been performed on plasma-surface interactions, although many important interactions occur on the surface. Most of these have involved surface analysis after etching or have simulated plasma conditions in beam experiments conducted under high vacuum. Such postetching or high-vacuum, nonplasma environments are necessary to allow conventional electron-detection-based surface analysis techniques to be used. To understand and better control etching processes, real-time surface diagnostic techniques are required that are not based on electron spectroscopy.

As with earlier, well-established gas-phase probes, optical diagnostic methods hold great promise for probing the surface during plasma processing.¹⁾ For example, infrared (IR) optical absorption is one technique that can be applied, and a study of etching of Si in a chlorine plasma has recently been published.²⁾ Surface IR absorption is weak, however, and Si-Cl vibrational frequencies are low, so that special wedged substrates, sometimes with buried metal layers, are required to obtain sufficient sensitivity. Recently, we reported a laser-desorption laser-induced fluorescence (LD-LIF) technique for measuring Cl and Br coverages on Si during etching in high-density Cl₂/HBr plasmas.^{3–5)} Laser pulses are used to heat the surface rapidly and desorb silicon monohalide molecules that are detected by LIF. The LD-LIF technique can be applied at the pressures typically used in plasma etching, or at higher pressures. When laser-induced thermal desorption (LITD) is used to study surface reaction kinetics in ultrahigh vacuum (UHV),^{6–9)} desorbing species are normally detected with a mass spectrometer. Recently, LITD with mass spectrometric detection has also been used to measure chlorine

and fluorine coverages during silicon plasma etching.¹⁰⁾ LD-LIF is capable of detecting coverages of < 0.1 monolayer in plasma environments with a time resolution of less than 0.02 s. We review work recently reported in refs. 3–5 on the use of LD-LIF to study the surface *in situ* during plasma etching of silicon, and also provide insights into the mechanism of the etching process that were drawn from these observations.

2. Experimental Methods

The experimental apparatus used in the laser desorption experiments is shown in Fig. 1. The plasma reactor consists of a helical resonator source (11.2 MHz, RF power to 300 W) and a stainless steel downstream chamber, along with two 100 G solenoid magnets.^{3–5, 11, 12)} The substrate stage is radio-frequency (RF)-biased (14.5 MHz) to achieve DC bias voltages of 0 to –120 V. The charge density above the Si(100) substrate (n type, P doped, 5–50 Ω · cm) in the downstream chamber was 1–2 × 10¹¹ cm^{–3} (as measured for argon plasmas). In some experiments the surface was analyzed by LD-LIF during etching in a pure Cl₂ plasma,^{3, 4)} while in others it was examined for Cl₂/HBr plasmas with the Cl₂/(HBr + Cl₂) ratio varied from 0 to 1.⁵⁾ Cl₂/HBr total flow rates of 2–17 sccm and pressures of 0.6–20 mTorr were used. The surface was also examined during exposure to Cl₂/O₂ plasmas.⁴⁾ The ion flux to the surface was measured with a Langmuir probe (PMT Fastprobe). The plasma potential was 50 V, independent of DC bias. Etch rates were measured by laser interferometry on polycrystalline Si films on 1000 Å SiO₂ atop Si(100) substrates. A UHV load-lock chamber connects the plasma reactor to a UHV chamber equipped for X-ray photoelectron spectroscopy (XPS), allowing samples to be transferred to this chamber after etching and analyzed without exposure to air.

The LD-LIF detection apparatus is mounted on the plasma chamber (Fig. 1). It consists of a XeCl excimer laser (308 nm), imaging optics to collect the fluorescence and a monochromator equipped with a photomultiplier tube. The laser passes through a focusing lens and a viewport at the top of the plasma source and irradiates a 2.6 × 6.2 mm region of the sample at normal incidence. The LD-LIF measurements were performed on unmasked

*Present address: Gasonics International, 2730 Junction Ave., San Jose, CA 95134, U.S.A.

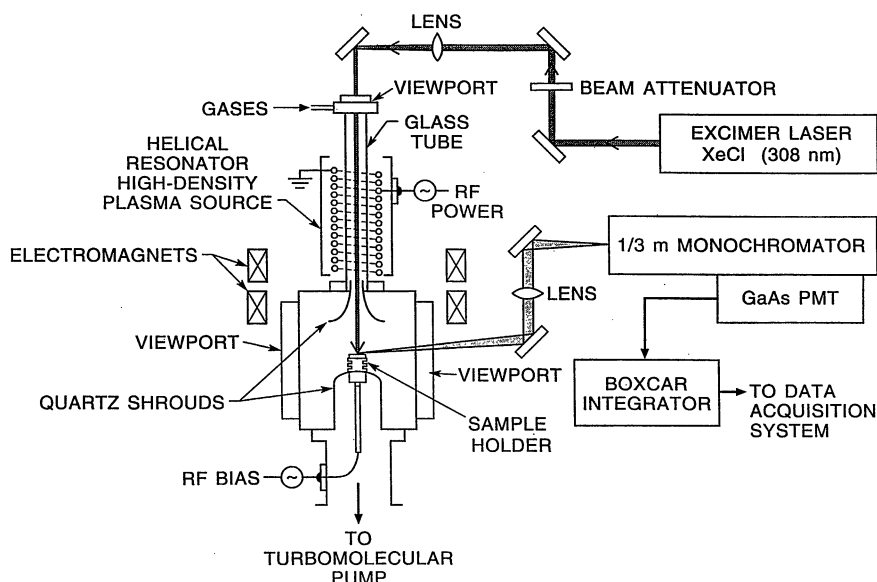


Fig. 1. Schematic depiction of the LD-LIF apparatus. The vacuum transfer and XPS chamber are not shown (from ref. 4.).

Si(100) samples *in situ* during etching. The XeCl laser heats the Si surface rapidly to near the melting point, and the tail of this ~ 15 -ns-long laser pulse can excite fluorescence from desorbing species. The fluorescence from the near-surface region is imaged onto the entrance slit of the monochromator. A boxcar integrator samples the emitted light immediately after the laser pulse. This collection system also enables analysis of the steady-state plasma-induced emission (PIE) and transient changes in the PIE due to laser-desorbed species (LD-PIE).

3. Observations

Three types of spectra are observed for Cl_2 plasmas, as shown in Fig. 2 (2500–3050 Å).³⁾ The steady-state PIE signal, without laser irradiation, shows features due to excited Si, Cl_2 , and SiCl ($\text{B}^2\Delta \rightarrow \text{X}^2\Pi_r$). The LD-LIF trace shows the fluorescence of species that are desorbed from the surface by the laser and are pumped to an excited electronic state by the tail of the same laser. Given the ~ 15 ns pulse length of the laser, LD-LIF can originate only from species desorbed from the surface before they collide with neutral and charged species in the plasma. The 308 nm radiation from the XeCl laser excites the $\text{B}^2\Sigma^+ (v' = 0) \leftarrow \text{X}^2\Pi_r (v'' = 3, 4)$ transitions in SiCl , leading to fluorescence from $\text{B}^2\Sigma^+ (v' = 3, 4) \rightarrow \text{X}^2\Pi_r (v'')$, as depicted in Fig. 2. The $\text{B}^2\Sigma^+$ state has a lifetime of 10 ns, so given this and the laser pulse length, LD-LIF is confined to a region within about $10 \mu\text{m}$ from the surface. Although 308 nm also can excite LIF from SiCl_2 , no fluorescence from SiCl_2 was observed. (This does not indicate that no SiCl_2 desorbs during laser heating since the detection efficiency for this emission is lower than that for SiCl .) With HBr present in the flow mixture, LD-LIF is also observed due to 308 nm excitation and subsequent emission in the $\text{SiBr B}^2\Sigma^+ - \text{X}^2\Pi_r$ band (see Fig. 7 below).

This LD-LIF signal peaked just above the surface in the time interval immediately after the laser pulse. A

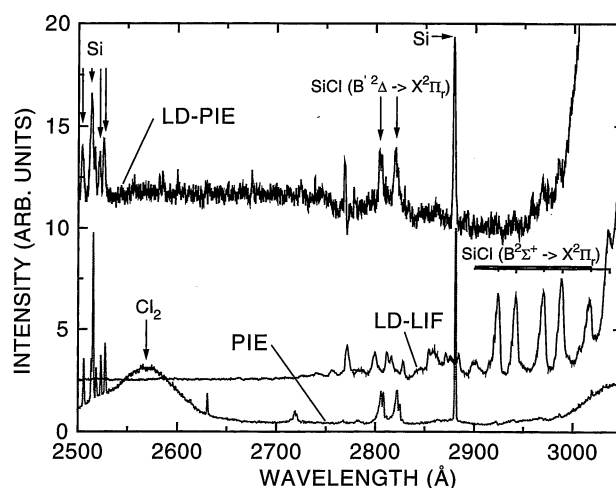


Fig. 2. Spectra during etching of Si(100) by Cl_2 , showing steady-state plasma-induced emission (PIE) and transient changes after laser desorption (0.5 J/cm^2) from emission (LD-PIE) and LIF (LD-LIF) (from ref. 3).

qualitatively different transient change was seen in the light viewed several mm above the surface, which is denoted as LD-PIE in Fig. 2. This change peaked several μs after the laser pulse, which is consistent with species leaving the surface with a mean speed of $\sim 1 \times 10^5 \text{ cm s}^{-1}$. LD-PIE spectral features similar to the Si and SiCl PIE features are observed. The LD-PIE emission may be due to SiCl along with other species that desorb from the surface; these desorbing species may be directly excited by electrons or may be collisionally transformed into other species in excited electronic states that then fluoresce.

The LD-LIF signals with the plasma on and off both depend on laser fluence in a manner that suggests a thermal desorption process. They have distinct threshold fluences with the plasma on [$\sim 0.20 \text{ J/cm}^2$ for both LD-LIF (SiCl) and LD-PIE (Si and SiCl)] and plasma off

$[\sim 0.35 \text{ J/cm}^2 \text{ for LD-LIF (SiCl)}]$, indicating that a more weakly bound layer forms when Si(100) is exposed to a Cl_2 plasma than when it is exposed to Cl_2 gas.³⁾ The LD-LIF signal saturates at fluences of $\sim 0.6 \text{ J/cm}^2$; in the experiments described below the surface layers were examined under such saturation conditions. Heat flow calculations suggest that the surface begins to melt at a fluence of 0.45 J/cm^2 at 308 nm.

With Cl_2 flow, the intensity of the SiCl LD-LIF signal increases by a factor of ~ 2.2 when the plasma is on, due to an increase in Cl coverage on the surface (Fig. 3, 5 Hz laser repetition rate).^{3, 4)} This figure also shows that the plasma and surface layer reach steady-state conditions in the time between laser pulses, 200 ms. For HBr flow, the SiBr LD-LIF increases when the plasma is turned on, indicating that the surface becomes more highly brominated with the discharge on.⁵⁾

The surface adlayers formed with and without the plasma on are stable after the laser irradiation is stopped, the plasma is extinguished (for plasma etching), and the gas is pumped away, as is seen by resuming laser irradiation several minutes later. For Cl_2 flow, the SiCl LD-LIF signals observed on the first pulse are close to the respective steady-state signals (Fig. 3), indicating that the chlorine coverage does not decrease significantly ($< 10\%$) during the pump-down.^{3, 4)} Continuous irradiation under these conditions leads to a rapid decay of the signal to an undetectable level. Roughly $1/e$ of the Cl is removed per laser pulse. These observations suggest that the SiCl_x adsorbed layer is stable after the plasma is extinguished, so, at least for this system, in-line XPS analysis is indicative of the steady-state surface during etching. Similar stability of the SiBr_x layer was observed during Si etching by HBr plasmas.⁵⁾

In chlorine plasmas the SiCl LIF signal is proportional to Cl coverage ($\text{SiCl}_{x(\text{ads})}$), as verified by XPS. This was shown by transferring samples to the analysis chamber after exposure to the plasma, with no laser irradiation during the last stage of the exposure, or following exposure to the laser and Cl_2 after turning the plasma

off. XPS indicates that the layer formed during plasma etching corresponds to a coverage of $1.0 \times 10^{15} \text{ Cl/cm}^2$.⁴⁾ High-resolution Si(2p) spectra revealed that Si mono-, di-, and trichlorides were present. The Cl(2p)-to-Si(2p) ratio was 1.9 times higher after plasma exposure than after exposure only to the laser and Cl_2 , in good agreement with the 2.2-fold increase in the LD-LIF signal when the plasma was turned on. Thus, at low laser repetition rates the LD-LIF method provides an instantaneous measure of chlorine coverage in the steady state. Analogous in-line XPS measurements for HBr plasmas give a Br coverage of $6.0 \times 10^{14} \text{ Br/cm}^2$.⁵⁾

Cl coverage was measured as a function of discharge power, pressure, and bias voltage for chlorine plasmas.⁴⁾ The dependence on RF power is shown in Fig. 4. The total Cl coverage increases rapidly with power and reaches a saturated level at a substantially lower power [$\sim 100 \text{ W}$] than does the etch rate or ion flux (saturated ion current) [$\sim 300 \text{ W}$]. This increase in coverage with power is ascribed to the increase in the formation of Cl atoms with increasing power, which is shown elsewhere to depend on power in similar manner.¹³⁾ The etch rate increases both with Cl coverage and ion flux at low power, and then is proportional to ion flux at the higher powers that are more typical of standard conditions in commercial high-density plasmas. Consequently, the etch rate under these latter conditions is limited by the ion-bombardment removal of product rather than by the supply of Cl to the surface. This is further supported by the observed pressure-independent Cl coverage and etch rate from 0.6–20 mTorr. Changing the DC bias of the substrate from 0 to -125 V linearly increases the LD-LIF signal, and consequently also the thickness of the chlorinated adlayer, by only $\sim 25\%$. Changing the DC bias from 0 to -90 V (ion energy from 50 to 140 eV) increases the etch rate by $\sim 60\%$ (Fig. 5).

The rate of surface chlorination can be determined by varying the laser repetition rate and Cl_2 pressure. A plot of Cl coverage as a function of repetition rate is shown in Fig. 6 for two pressures. At low pressure and high repetition rate the laser irradiation is removing surface chlorine faster than the plasma can supply it. A first-order rate coefficient of $8.1 \times 10^4 \text{ s}^{-1} \text{ Torr}^{-1}$ was de-

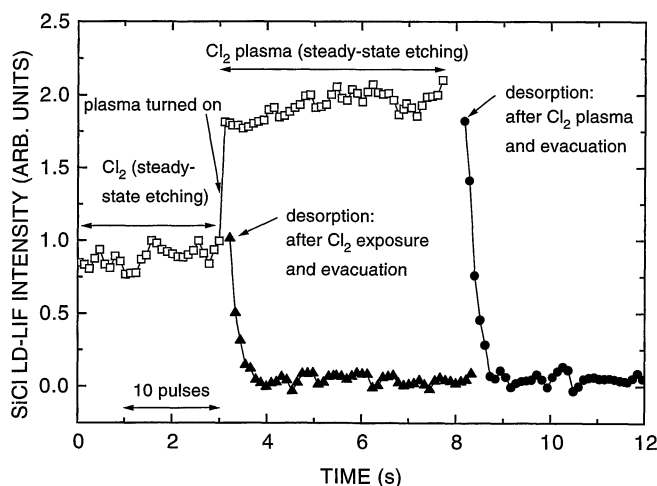


Fig. 3. LIF intensity of laser-desorbed SiCl (2924 Å) showing changes when the plasma is turned on and after pump-down (with the plasma initially either on or off; pump-down time is not shown) (from ref. 3).

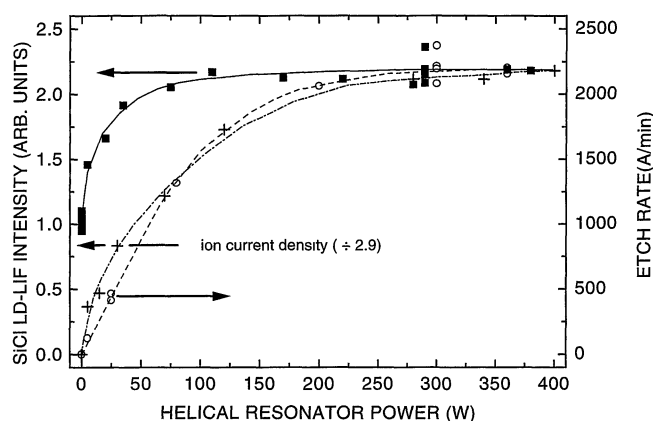


Fig. 4. SiCl LD-LIF signal intensity (1 arb. unit = $5 \times 10^{14} \text{ Cl/cm}^2$), Si etch rate, and saturated ion density (which should be normalized to 6.3 mA/cm^2 at 400 W) vs RF power (from ref. 4).

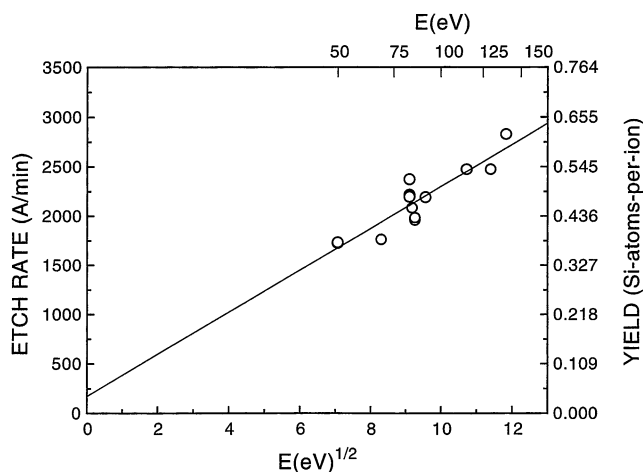


Fig. 5. Si etch rate and sputtering yield vs ion energy, with the ion energy equal to the plasma potential (50 V) minus the DC bias voltage (from ref. 4).

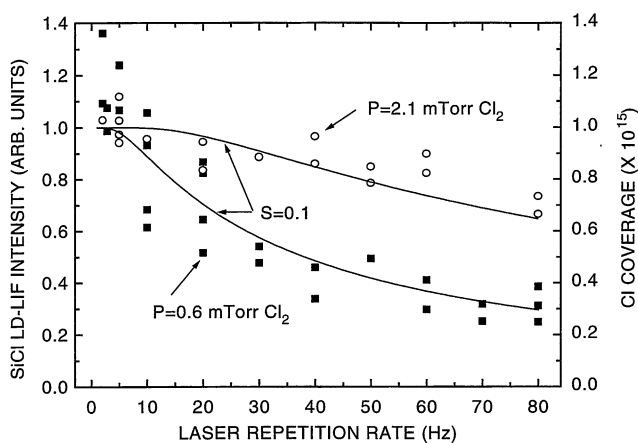


Fig. 6. SiCl LD-LIF signal intensity (converted to Cl coverage on the right-hand axis) vs laser repetition rate during Cl_2 plasma etching of Si(100), with model predictions assuming a sticking coefficient of $S=0.1$ (adapted from ref. 4).

rived from the dependence of the LD-LIF signal on laser repetition rate and pressure. This indicates that chlorination occurs rapidly with respect to the time required to etch one monolayer, at pressures as low as 0.5 mTorr. The predominant species impinging on the surface is believed to be Cl atoms.¹³⁾ If the other chlorine species are ignored, then using a simple Langmuir adsorption model gives a sticking coefficient of ~ 0.1 , as indicated by the fitted solid curves in Fig. 6.

Similar observations can be made in plasmas containing HBr, using 308 nm LD-LIF for detecting desorbed SiBr.⁵⁾ In mixed Cl_2/HBr plasmas, this LD-LIF scheme simultaneously detects desorbed SiCl and SiBr, as shown in Fig. 7. For these mixtures the surface coverages of Cl and Br are simply proportional to the total respective halogen content of the feed gas (Fig. 8). This is seen quantitatively by the in-line XPS measurements and semiquantitatively by the *in situ* LD-LIF measurements. The total halogen coverage decreases with increasing HBr, reaching a saturated Br coverage in pure HBr plasmas that is 0.6 times the saturated Cl coverage

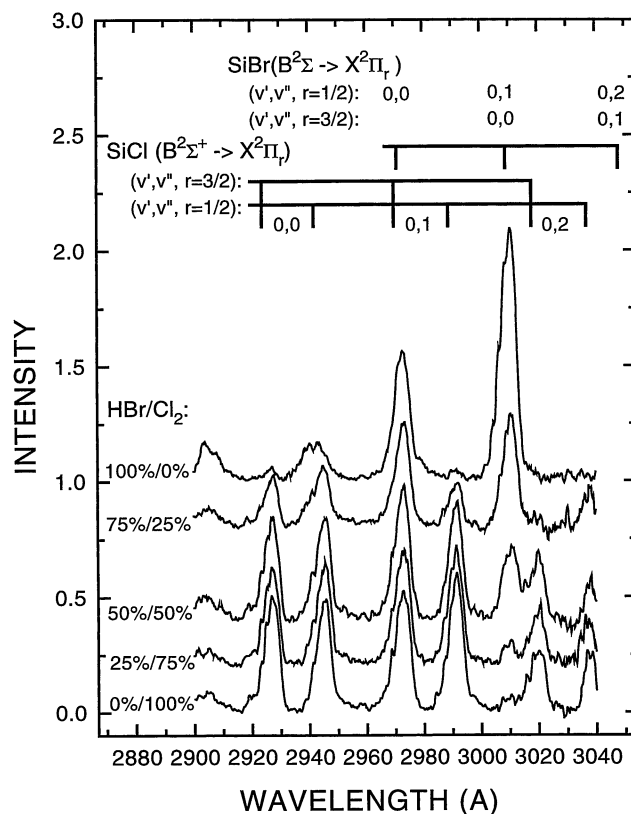


Fig. 7. Laser-desorption, laser-induced fluorescence spectra of SiCl and SiBr recorded during etching of Si(100) by Cl_2/HBr plasmas as a function of gas ratio (from ref. 5).

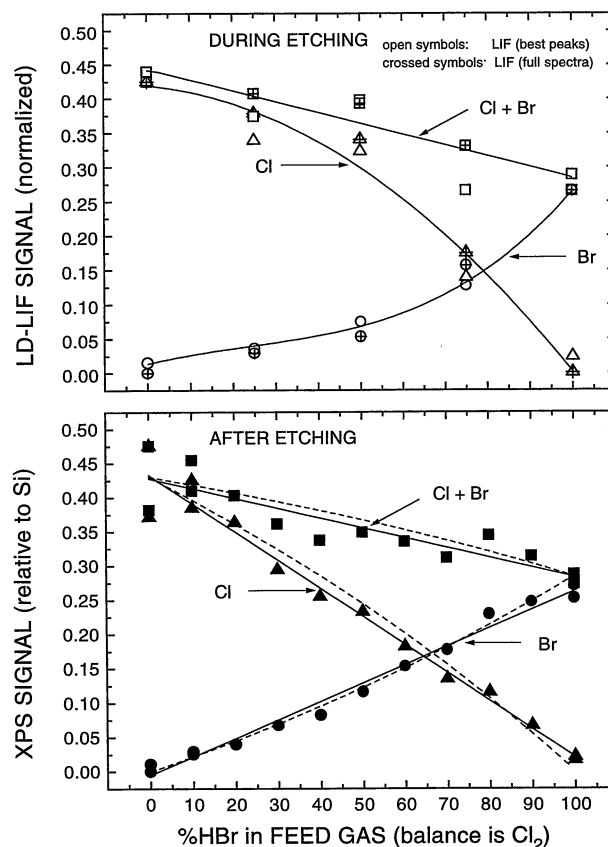


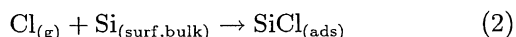
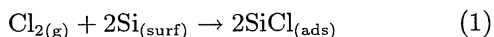
Fig. 8. Relative fractions of Cl and Br on the surface during plasma etching of Si(100) by Cl_2/HBr plasmas as functions of gas ratio from (top) the LD-LIF signals from SiCl and SiBr and (bottom) in-line XPS (from ref. 5).

in Cl_2 plasmas, as determined by in-line XPS. The similar reduction in the Si etch rate in HBr plasmas is likely due to this reduced halogen coverage.

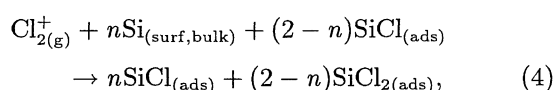
Both the etch rate and the LD-LIF signal ($\text{SiCl}_{x(\text{ads})}$ coverage) were observed to decrease dramatically for Cl_2/O_2 mixtures with an O_2 fraction $> 20\%$.

4. Discussion

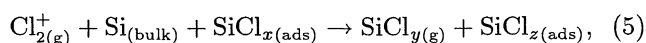
The steps in the etching of Si in this high-density chlorine plasma include chlorination by neutral species,



and ions,



where $n = 0, 1$, or 2 , and ion sputtering of SiCl_x ,



where $x + 2 = y + z$ if no Cl or Cl_2 sputters or recoils, and charge conservation is not explicitly noted.

In this plasma, the flux of Cl to the surface is apparently much larger than the fluxes of Cl_2 and Cl_2^+ ,¹³⁾ so reactions (2) and (3) probably dominate surface chlorination. From Fig. 6, it is seen that for pressures above ~ 0.5 mTorr, the $\text{SiCl}_{x(\text{ads})}$ layer reaches saturated coverage much faster than the time required to etch one monolayer (40 ms) for typical etching conditions (~ 300 W RF power). Therefore, the rate of ion bombardment is the limiting factor in the rate of etching in these pressure regimes.

The etch rate increases faster with DC bias than does the LD-LIF signal ($\text{SiCl}_{x(\text{ads})}$ layer coverage). This means that increasing the ion speed towards the substrate increases the probability of removing species from the adlayer (reaction (5)). Using the measured plasma potential of 50 V, and the measured etch rate vs bias voltage, the number of Si atoms sputtered from the surface per incident ion increases from 0.38 at 50 eV to 0.60 at 125 eV, as seen in Fig. 5.

Adding HBr to the Cl_2 flowing into a discharge can improve the anisotropy of the Si etch and the selectivity of the Si etch over SiO_2 ; however for large HBr fractions it also slows the etching rate. For this plasma, the etch rates for pure Cl_2 and pure HBr plasmas (280 Watts, -35 V DC bias) are 2170 and 1330 Å/min, respectively, which are seen to be proportional to the respective saturated coverages of Cl and Br, as determined by XPS. Therefore, the rate of forming volatile silicon bromides by ion bombardment is slower than that for silicon chlorides, mainly because there is less Br available on the surface during HBr etching than Cl during Cl_2 etching.

Oxygen is often added to Cl_2 plasmas to improve the selectivity of Si with respect to SiO_2 . Since $\text{SiCl}_{x(\text{ads})}$ and the etch rate were both observed to decrease dramatically for Cl_2/O_2 flows with O_2 fractions $> 20\%$, it appears that for such O_2 -rich mixtures the formation of

$\text{SiO}_{x(\text{ads})}$ begins to become important, and inhibits the etching process.

The LD-LIF data presented in Fig. 3 for chlorine plasmas (and analogous data for HBr plasmas⁵⁾) suggest that the surface layer during etching does not change appreciably when the plasma is turned off. Fast thermal desorption of even $\sim 1/4$ monolayer of surface adsorbates that would desorb as SiCl during laser heating would have been observed in the LD-LIF measurements depicted in Fig. 3. Moreover, the fluence thresholds for the Si and SiCl LD-PIE signals were found to be the same as that for SiCl LD-LIF. Since SiCl and other SiCl_x species probably contribute to the LD-PIE signals for Si and SiCl, a rapidly desorbing layer containing Si and/or Cl would likely mean a lower fluence threshold for LD-PIE. (Using real-time ellipsometry, Oehrlein¹⁴⁾ did not observe a volatile overlayer during plasma etching with fluorinated etchants, which justified his use of in-line XPS analysis of the surface.)

Silicon etches at a rate of ~ 40 Å/s under typical conditions (300 W RF, -32 V bias), so 8 Å (5 monolayers) is etched between laser pulses (5 Hz). This means that in LITD, each laser pulse interrogates a surface representative of one during steady-state etching, independent of the heating, and possible melting, of the surface by the previous pulse. (The surface of the Si(100) wafer during steady-state plasma etching is probably highly disordered.) Possible transient changes to the plasma due to the laser, by, for example, LITD, LIF, photodetachment and photodissociation, would decay before the next pulse. Furthermore, since the photon energy (4.0 eV) is less than the work function of silicon (~ 5 eV), electron emission from the surface due to the laser can be ignored. While these attributes make LD-LIF a valuable *in situ* probe for understanding a process, the inherently invasive nature of the laser desorption process, along with the complexity of the laser system, makes it unsuitable as a real-time probe for control of plasma etching during manufacturing.

Although the intensities of both the LD-LIF and LD-PIE spectra are expected to be linearly proportional to the flux of the desorbed species, monitoring LD-LIF is preferred because it gives a stronger signal. Moreover, the excitation process in LD-LIF depends on the laser intensity, which can be controlled, while the excitation process in LD-PIE depends on plasma conditions which may vary in a parametric study. However, when the laser used to induce desorption cannot excite LIF in the desorbed species and LIF detection with a second laser is inconvenient or not possible (as for larger radicals and molecules), LD-PIE can be used to probe the desorbed species.

5. Concluding Remarks

Laser-induced thermal desorption (LD), combined with laser-induced fluorescence (LIF) detection, was used to study the etching of single-crystal Si(100) in a high-density, low-pressure Cl_2/HBr -containing helical resonator plasma, with supporting in-line XPS measurements. One major finding of these studies is that during etching the Si surface rapidly becomes covered with a

stable (in vacuum) saturated layer of about 2 monolayers of chlorine in a Cl_2 plasma and about 1 monolayer of bromine in an HBr plasma. The layer consists of silicon mono-, di-, and trihalides. In Cl_2 plasmas, the Cl coverage increases with ion energy, but is nearly independent of pressure (0.5–20 mTorr). Chlorination occurs rapidly with respect to the time required to etch one monolayer, at pressures as low as 0.5 mTorr. Consequently, the etching rate is limited by the ion flux, and not the neutral flux under these conditions. Still, at lower RF powers, the surface coverage is seen to vary with power. In mixed Cl_2/HBr plasmas, the coverages of Cl and Br are simply proportional to the total halogen content in the respective feed gas.

LD-LIF does not detect all desorbing species, and it may not even be able to detect the major desorption product. In these experiments, however, the detected species (SiCl or SiBr) appears to be a primary product that desorbs during laser heating. Although LD-LIF is invasive, it is still a quantitative *in situ* diagnostic of the surface coverage during steady-state etching, which can also be used to track the change in surface coverage in response to changes in the plasma conditions. Furthermore, LD-LIF can be used to validate the use of in-line XPS analysis for accurate determination of the surface coverage, as was done here for the $\text{Si}/\text{Cl}_2/\text{HBr}$ etching system.

Acknowledgement

One of the authors (IPH) would like to thank the support provided by NSF grant DMR-94-11504.

- 1) I. P. Herman: *Optical Diagnostics for Thin Film Processing* (Academic, San Diego, 1996).
- 2) K. Nishikawa, K. Ono, M. Tidu, T. Oomori and K. Namba: 1994 Dry Process Symp., p. 105.
- 3) I. P. Herman, V. M. Donnelly, K. V. Guinn and C. C. Cheng: Phys. Rev. Lett. **72** (1994) 2801.
- 4) C. C. Cheng, K. V. Guinn, V. M. Donnelly and I. P. Herman: J. Vac. Sci. & Technol. A **12** (1994) 2630.
- 5) C. C. Cheng, K. V. Guinn, I. P. Herman and V. M. Donnelly: J. Vac. Sci. & Technol. A **13** (1995) 1970.
- 6) H. Hartwig, P. Mioduszewski and A. Pospieszczyk: J. Nucl. Mater. **76** (1978) 625.
- 7) R. B. Hall and A. M. DeSantolo: Surf. Sci. **137** (1984) 421.
- 8) R. B. Hall, A. M. DeSantolo and S. J. Bares: Surf. Sci. **161** (1985) L533.
- 9) S. M. George: *Investigations of Surfaces and Interfaces*, eds. B. W. Rossiter and R. C. Baetzold (Wiley, New York, 1993) Part A, Chap. 7, p. 453.
- 10) M. Nakamura, K. Otuka and K. Karahashi: presentation PS-TuM4, 42nd National Symp. of the American Vacuum Society, Oct. 16–20, 1995, Minneapolis.
- 11) K. V. Guinn and V. M. Donnelly: J. Appl. Phys. **75** (1994) 2227.
- 12) K. V. Guinn, C. C. Cheng and V. M. Donnelly: J. Vac. Sci. & Technol. B **13** (1995) 214.
- 13) V. M. Donnelly: to be published in J. Vac. Sci. & Technol. A **14** (1996).
- 14) G. S. Oehrlein: J. Vac. Sci. & Technol. A **11** (1993) 34.